

---

# ADAPTIVELY CONTROLLABLE DIFFUSION MODEL FOR EFFICIENT CONDITIONAL IMAGE GENERATION

---

**Yucheng Xing, Xiaodong Liu, Xin Wang**

Department of Electrical and Computer Engineering

Stony Brook University

Stony Brook, NY 11794, USA

{yucheng.xing, xiaodong.liu, x.wang}@stonybrook.edu

## ABSTRACT

With the development of artificial intelligence, more and more attention has been put onto generative models, which represent the creativity, a very important aspect of intelligence. In recent years, diffusion models have been studied and proven to be more reasonable and effective than previous methods. However, common diffusion frameworks suffer from controllability problems. Although extra conditions have been considered by some work to guide the diffusion process for a specific target generation, it only controls the generation result but not its process. In this work, we propose a new adaptive framework, *Adaptively Controllable Diffusion (AC-Diff) Model*, to automatically and fully control the generation process, including not only the type of generation result but also the length and parameters of the generation process. Both inputs and conditions will be first fed into a *Conditional Time-Step (CTS) Module* to determine the number of steps needed for a generation. Then according to the length of the process, the diffusion rate parameters will be estimated through our *Adaptive Hybrid Noise Schedule (AHNS) Module*. We further train the network with the corresponding adaptive sampling mechanism to learn how to adjust itself according to the conditions for the overall performance improvement. To enable its practical applications, AC-Diff is expected to largely reduce the average number of generation steps and execution time while maintaining the same performance as done in the literature diffusion models.

**Keywords** Diffusion Model · Conditional Image Generation · Input-Adaptive Model

## 1 Introduction

Artificial intelligence generated content (AIGC) has been an important and popular topic in the machine learning community. On the one hand, the creativity shown by the generative models is a critical indicator to measure the level of artificial intelligence. On the other hand, generated contents could help improve the performance of other machine learning tasks by augmenting data for model training. Starting from auto-regressive model [1], many branches of generative models have been studied, such as Normalizing Flows [2], VAE [3], and GAN [4]. Particularly, diffusion models [5] have been explored recently and proven to outperform all other generative methods with their more stable training processes.

Despite the potential, diffusion models suffer from three major limitations that prevent their practical applications. First, traditional diffusion models are unconditional with an uncontrollable generation process, thus their generation results are almost random without constraints. Second, the pre-calculated diffusion rate parameters (i.e. the noise schedule of the diffusion process) are fixed and kept the same for all kinds of generation tasks, so the variety of generated images only depends on the sampling randomness but not to meet different generation demands. Last and most importantly, the number of generation steps is pre-defined and kept the same regardless of the contents to be generated. Such a setting will not only bring unnecessary diffusion steps for simple contents but also leave complex contents not fully generated. To understand these constraints, we can compare the generation process to hand-carving. In the latter case, the outline is first generated and the details are then gradually added, and the number of steps required to generate an apple must be much fewer than that needed to produce a fully fledged bird.

To make the models more controllable, additional information has been introduced [6, 7, 8, 9, 10, 11, 12, 13] to guide the generation process towards the target, using constraints such as category labels, texts and images. Although a guidance is applied in each method to improve the generation quality, none of these methods can fully “control” the generation process to both adapt the length of the diffusion process and the diffusion rate parameters (or noise schedule) based on input conditions. To speed up the diffusion models, intuitive methods such as sub-sampling [14, 15, 16, 17, 18] and early-stop [19, 20, 21] are used. These strategies either blindly reduce the steps uniformly without considering the contents, or adapt the step sizes based on step-wise estimation with a high amount of extra calculation. Instead, we propose to develop a sample-wise adaptation to find the number of steps needed to generate a sample image only at the very beginning of its diffusion process.

In light of these problems, we propose a new controllable diffusion framework, named as *Adaptatively Controllable Diffusion (AC-Diff) Model*, which consists of two major modules: *Conditional Time-Step (CTS)* and *Adaptive Hybrid Noise Schedule (AHNS)*. Before entering the actual diffusion process, according to the application demands, the input text prompts and additional image conditions are fed into the CTS module to calculate the length (i.e., the number of diffusion time-steps) of the process. In order to work with the dynamic diffusion steps, rather than using fixed diffusion rate parameters as done in the literature, the parameters are generated through adaptive noise re-scheduling by the AHNS module. In addition, since the process in our model is dynamic, we will also design an adaptive sampling mechanism during training such that the model can better learn how to well adjust its generation process from the conditions in practical applications.

In summary, our contributions in this paper are three-folded:

- We propose a new dynamic framework for diffusion model, which is adaptively controlled by input prompts and additional conditions such that the length of diffusion process can be adjusted according to demands;
- To better adapt to varying diffusion process, commonly used pre-calculated diffusion parameters are replaced by dynamic ones generated by sample-wise noise re-scheduler each time;
- Besides the generation phase, we also integrate the input conditions during the training phase. Instead of using a pre-trained unconditional model, we design an adaptive sampling mechanism to train our diffusion model.

The remaining of this paper is organized as follows: In Sec. 2, we will overview the literature works related to diffusion models. The details of our model will be given in Sec. 3 and its effectiveness is going to be proved in Sec. 4 through experiments. Finally, we will summarize the whole work in Sec. 5.

## 2 Related Work

### 2.1 Conditional Diffusion Model

In traditional unconditional diffusion models, the generation results are stochastically sampled from the distribution learnt from the training dataset step-by-step, which are lack of outside control. On the contrary, many conditional diffusion models are explored recently to trade diversity for fidelity, producing high quality samples related to some specific objects, rather than covering the whole distribution. Common conditions used to control the generation process include category labels [6, 7, 22], texts [8, 9, 10, 23, 24, 25, 26] and images [10, 11, 27, 28, 29, 30]. The control methods can be divided into two groups: 1) Guidance-based, where a separate model is trained to take the intermediate images generated by the diffusion model as input to calculate the similarity with given conditions, and the gradients work as the score to revise the distribution for the next step sampling; 2) Directly combining the condition by embedding it into the generated results in the latent space. In the first group, Dhariwal and Nichol [6] modify the unconditional diffusion model with additional classifier for image synthesis, based on which Ho and Salimans [7] propose classifier-free guidance where the same diffusion model is only trained with score estimators with and without labels but not using the extra classifiers. To deal with limited labels during conditional training, You *et al.* [22] propose to alternatively train the classifier and the diffusion model. CLIP [31] model is commonly used in [8, 9, 10] to compare the intermediate outputs of the diffusion model with given text conditions to provide the guidance for the generation process. Liu *et al.* [10] also train an image encoder to take the image conditions into consideration. The same idea is utilized by Voynov *et al.* [11] where the edge map estimator is trained to let the given sketch image to guide the generation. A conditional diffusive estimator is used in [28] to diffuse both conditions and generated images and match them. Instead of training, Yu *et al.* [27] propose a training-free framework where an arbitrary pre-trained model is used to extract features from both generated images and conditions to calculate an energy score. As the second group of methods, in order to reduce the computational complexity, Rombach *et al.* [32] first propose to apply the diffusion process to latent features, and extra conditions are encoded and integrated with them through cross-attention mechanism, which is also widely used in [9, 23, 24]. The conditional embedding can also be directly concatenated with generated

latent features from diffusion models as did in [25, 26]. In Zhang *et al.*’s work [29], a copy of trained diffusion model is used to encode edge-based image conditions, which are combined with the original latent diffusion features using newly designed zero-convolution operations. It is extended by Qin *et al.* [30] such that the condition image is not limited to canny edge and the like. Besides, scene graphs [12] and layout [13] are also used as conditions to be added through cross-attention or concatenation. In Singh *et al.*’s work [33], the condition works on the input noise generated through inverted gradient. For these conditional models, the conditions are mainly related to the reverse diffusion process. To make it more flexible, Zhang *et al.* [34] propose to introduce conditions into the forward process as well. For both types of methods proposed by the literature work, although conditions are added to control the generation results, the generation process, especially the diffusion steps needed, is not affected by the conditions. Instead, our model is aims to fully control the diffusion model, both the process and the results.

## 2.2 Efficient Diffusion Sampling

No matter score-based models [35] or diffusion-based models [5], iterative generative models add noise that the data distribution gradually collapses into a simple noise distribution and reverse this process to generate high quality samples. Although they show impressive performance, these models suffer from high computational cost, typically requiring hundreds or thousands iterations for each sample, which prevents them from being used in practical applications. To speed up the diffusion models, intuitive ways include sub-sampling [14, 15, 16, 17, 18] and early-stop [19, 20, 21]. On the one hand, it’s believed in previous methods that there is a decoupling between the schedules applied for training and for inference, so the number of steps used during the inference phase can be different from those in training. Specifically, Nichol and Dhariwal [14] adopt even distance sub-sampling of the total steps with learnt noise variance as a combination of the upper and lower bounds for each step, while Watson *et al.* [15] use dynamic programming algorithm to select the sub-sequence of steps to optimize the evidence lower bound. Song *et al.* [16] generalize traditional DDPMs [5] through a non-Markovian process to realize the jump among diffusion steps, which is further expanded by Watson *et al.* [17]. In San-Roman *et al.*’s work [18], the output after each step is utilized to estimate the amount of noise in data, so that fewer steps are scheduled in the generation process. On the other hand, since only the first few steps of the diffusion process contribute the most, some methods try to truncate the process and start the generation from a non-Gaussian distribution. In [20], Lyu *et al.* use an extra generative model, such as VAE [3], to first obtain an initial noisy image from the standard Gaussian distribution, and a normal diffusion process is applied on top of the intermediate image to get the final result. Zheng *et al.* [21] further omit the extra generative model and only use the same diffusion model to generate the initial image from total noise in one step, which is followed by a denoising process as usual. However, we notice that no matter sub-sampling or early-stop, these methods keep the total number of steps in the generation process the same for all target images. The possible speed-up brought by the difference among generation contents is neglected, while a uniform number of diffusion steps may also compromise the generation quality for complex images if the steps are blindly reduced. Actually, according to Song *et al.*’s research [36], the diffusion process can be regarded as a discretization of a continuous stochastic process, such that generation results can be obtained by solving the corresponding stochastic differential equations (SDEs). Meanwhile, they propose that it can be accelerated by solving probability flow ordinary differential equations (PF-ODEs) which have the same marginal distribution with SDEs. Therefore, a branch of works [37, 38, 39, 40, 41, 42, 43] start focusing on finding out much more efficient numerical solvers. The studies in [39, 40] conduct step adjustments according to the error-check among solvers of different orders after each iteration. These adaption strategies are different from ours since their step sizes are adapted based on the step-wise checking and decision, which require too much extra calculation, while our adaption is sample-wise and only needs the extra calculation once at the very beginning of the diffusion process. Furthermore, distillation technique is used in [44, 45, 46] to train a student model using fewer sampling steps, such that multiple original diffusion steps can be integrated into one step in it. The additional training needed in these methods incurs a high cost.

## 3 Methodology

The framework of the proposed AC-Diff Model is shown in Fig. 1. Specifically, different from a common conditional diffusion model, it contains an extra *Conditional Time-Step (CTS) calculator* and a corresponding *Adaptive Hybrid Noise Schedule (AHNS) module*. In the remaining of this section, we will discuss each module in details.

### 3.1 Conditional Time-Step (CTS) Calculation

In most previous diffusion-based generation methods, the diffusion algorithms progressively sample from noise distribution to generate images from complete noise. The whole process usually takes  $T$  iterations or time steps (Fig. 2 (a)), with  $T$  pre-defined and fixed regardless of the contents to be generated. Intuitively, the length of the generation process should adapt to inputs and conditions according to the complexity of contents to generate, as in Fig. 2 (b).

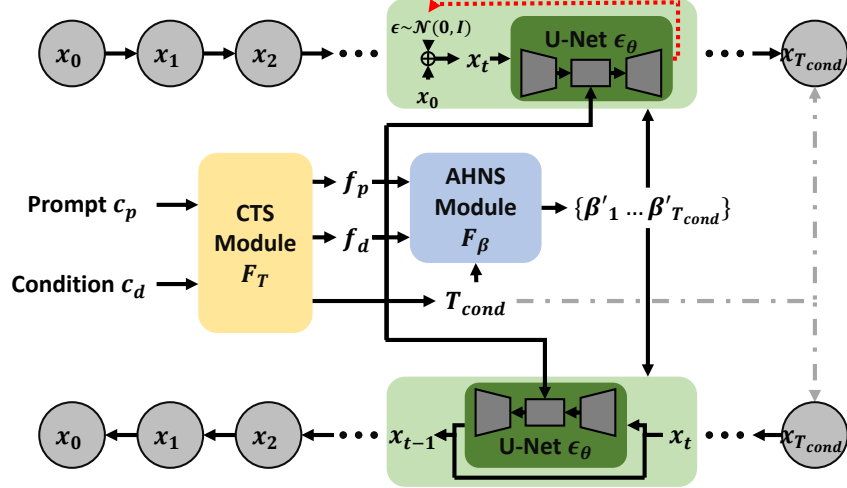


Figure 1: The framework of our AC-Diff model.

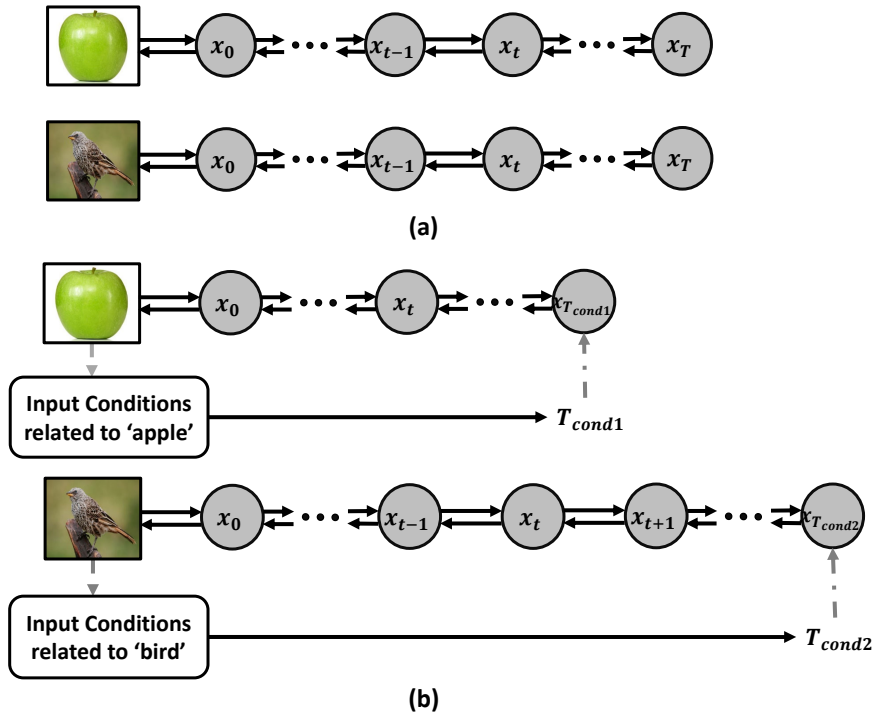


Figure 2: Illustration of adaptive diffusion length. (a) fixed length in previous methods. (b) adaptive length in our model.

To achieve such an adaptation, our CTS module  $F_T(\cdot)$  will adjust the number of diffusion steps  $T_{cond}$  according to the input  $c_p$  and condition  $c_d$ :

$$T_{cond}(c_p, c_d) = F_T(c_p, c_d), \quad (1)$$

where the input text prompts  $c_p$  may be category names and descriptions, and the image conditions  $c_d$  can be segmentation maps, outlines or sketches. As shown in Fig. 3, the CTS module contains the following parts:

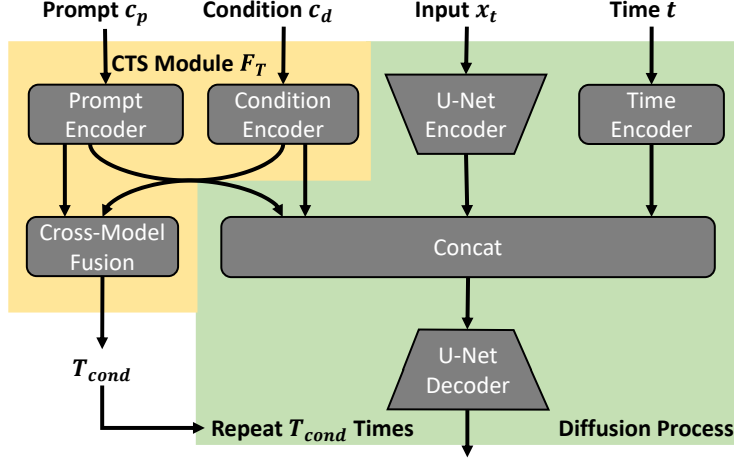


Figure 3: Illustration of our CTS module.

- **Prompt Encoding:** In our implementation, we use the standard text transformer of a pre-trained CLIP [31] model as the text encoder  $E_p(\cdot)$  to extract the prompt embedding. The process of text prompt embedding can be expressed as

$$f_p = E_p(c_p) = \text{Transformer}(c_p). \quad (2)$$

- **Condition Encoding:** Extra conditions in this paper mainly mean extra image-type clues, such as the sketch, outline, segmentation map or low-resolution image. To obtain the embedding from image conditions, we utilize the visual transformer (ViT) [47]  $E_d(\cdot)$  (also from a pre-trained CLIP model), whose encoding process is

$$f_d = E_d(c_d) = \text{ViT}(c_d). \quad (3)$$

- **Cross-Model Fusion:** With the prompt embedding  $f_p$  from the language model and the condition embedding  $f_d$  from the visual model, a cross-model fusion is needed to take both of them into consideration to get the final estimation of the time-step of the diffusion process. Since the original CLIP model is trained with paired texts and images, the extracted prompt embedding  $f_p$  and condition embedding  $f_d$  from Eq. (2) and Eq. (3) are mapped into a multi-model embedding space, and can be directly concatenated together. In our model, a simple two-layer multi-layer perception (MLP) model  $G_T$  is introduced to take the concatenation of  $f_p$  and  $f_d$ , and we can express the process as

$$T_{cond}(c_p, c_d) = G_T([f_p, f_d]) = \text{MLP}([f_p, f_d]). \quad (4)$$

Therefore, we can rewrite the conditional time-step calculation process in Eq. (1) as

$$\begin{aligned} T_{cond}(c_p, c_d) &= F_T(c_p, c_d) \\ &= G_T([E_p(c_p), E_d(c_d)]). \end{aligned} \quad (5)$$

Besides the semantic complexity calculated above, we further incorporate another spatial complexity ratio  $r_s$  according to the high-frequency information in the given image condition, to modulate the time-step obtained. Specifically, given the sketch (or edge map) of the image to be generated, we apply the information entropy on it by

$$r_s = - \sum_{x \in c_d} p(x) \log p(x), \quad (6)$$

where  $x$  is the pixel value in the conditional image. Such an entropy has been widely used in image-related fields for complexity measurement [48, 49, 50]. Then the final conditional time-step is  $T_{cond} = r_s * T_{cond}$ .

We would like to emphasize that this conditional calculation of the number of time-steps is only needed once for each new image to generate. The text prompt embedding and the image condition embedding are also going to be used for the image generation as done by previous conditional diffusion models. We expect the extra time taken by the simple cross-model fusion is negligible.

### 3.2 Adaptive Hybrid Noise Schedule (AHNS)

In common diffusion schemes, the noise schedule, controlled by a sequence of noise rate parameters  $\{\beta_1, \dots, \beta_T\}$ , is created manually and fixed. Some literature studies decouple the training and generation, and try to down-sample the number of diffusion steps in the reverse path to accelerate the generation process by choosing a subset of parameters  $\{\beta_{t_i} | i \in [1, K] \& \{t_1, \dots, t_K\} \subseteq \{1, \dots, T\}\}$ . The effectiveness of these schemes is built on the assumption that any clean image will become a pure Gaussian distribution in the forward diffusion process by gradually adding noise according to the schedule  $\{\beta_1, \dots, \beta_T\}$  in  $T$  iterations, but the reverse generation process might only contain a subset of these  $T$  steps.

In our framework, instead of using a fixed  $T$ , we believe that the length of the forward diffusion process  $T_{cond}$  taken to convert an input to a total noise should be conditioned on the complexity of the input, which is described by text prompts and image conditions. In other words, previous fixed- $T$  assumption is too strict and can be replaced by an adaptive one. Therefore, rather than just making a sub-sampling among  $\{\beta_1, \dots, \beta_T\}$ , we propose to also adjust the noise schedule  $\{\beta'_1, \dots, \beta'_{T_{cond}}\}$  during the training for better adapting to the conditional process length. Specifically, as shown in Fig. 4, our AHNS module includes two parts:

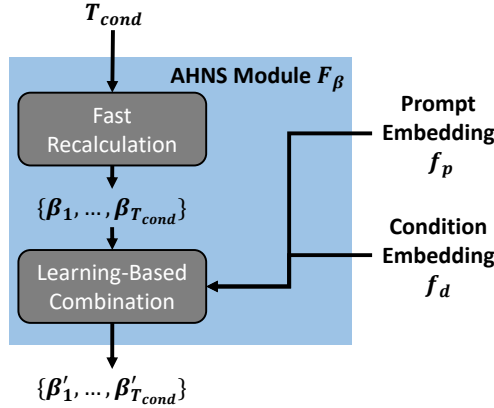


Figure 4: Illustration of our AHNS module.

- **Fast Recalculation:** According to study [14], the reasonable range of  $\beta$  is very small and hard for any model to directly predict. Just as done in DDPM [5], most of the current noise schedule set the extremums  $\beta_{min}$  and  $\beta_{max}$  as two predefined small values, and interpolate the remaining values according to some given schedule. In our design, we need to recalculate the set of diffusion parameters corresponding to the dynamic  $T_{cond}$  for each target image to be generated, and we don't want to add much more extra calculations. Therefore, we use a fast recalculation method in our model. That is, given a conditional maximum diffusion step  $T_{cond}$ , we just use a scheduler  $S(\cdot)$  to re-calculate the diffusion parameter sequence according to the updated extreme values modulated by the complexity ratio  $r_s$  as

$$\{\beta_1, \dots, \beta_{T_{cond}}\} = S(T_{cond}, \beta_{min}/r_s, \beta_{max}/r_s), \quad (7)$$

where  $S(\cdot)$  can be in any form such as linear, quadratic or sigmoid.

- **Learning-Based Combination:** As discussed in [51, 5], suppose the noise added in the  $t_{th}$  step is  $\epsilon_t \sim \mathcal{N}(\mu_t, \sigma_t^2)$ ,  $\beta_t$  and  $\tilde{\beta}_t = \frac{1-\bar{\alpha}_{t-1}}{1-\bar{\alpha}_t} \beta_t$ , where  $\alpha_t = 1 - \beta_t$  and  $\bar{\alpha}_t = \prod_{s=1}^t \alpha_s$ , correspond to the upper and lower bounds of the noise variance  $\sigma_t^2$  on the reverse process entropy. To make the schedule more content-adaptive, we propose to learn a conditional combination between  $\beta_t$  and  $\tilde{\beta}_t$ , i.e. the final variance of Gaussian noise to be added is

$$\sigma_t^2 = \beta'_t = \lambda \beta_t + (1 - \lambda) \tilde{\beta}_t, \quad (8)$$

where  $\lambda$  is the output from a simple MLP model  $G_\beta(\cdot)$  given the prompt embedding  $f_p$  and the condition embedding  $f_d$  from Sec. 3.1.

In formula, we can express the whole adaptive hybrid noise scheduling process as

$$\begin{aligned} \beta'_t &= \lambda \beta_t + (1 - \lambda) \tilde{\beta}_t \\ &= G_\beta([f_p, f_d]) \beta_t + (1 - G_\beta([f_p, f_d])) \frac{1 - \prod_{s=1}^{t-1} (1 - \beta_s)}{1 - \prod_{s=1}^t (1 - \beta_s)} \beta_t, \end{aligned} \quad (9)$$

where  $\beta_t \in \{\beta_1, \dots, \beta_{T_{cond}}\}$  are obtained from Eq. (7).

### 3.3 Training Phase – Forward Diffusion Process

Previously, in the training phase, given a noise  $\epsilon_t$ , the goal of the model is to estimate the added noise  $\epsilon_\theta(x_t, t)$  so as to minimize the objective

$$\mathbb{E}_{t \in [1, T]} \|\epsilon_t - \epsilon_\theta(x_t, t)\|^2, \quad (10)$$

where  $x_t$  is the noisy version from the clean image  $x_0$  by adding the noise according to the predefined diffusion rate parameter as

$$x_t = \sqrt{\bar{\alpha}_t} x_0 + \sqrt{1 - \bar{\alpha}_t} \epsilon_t, \quad (11)$$

and  $\bar{\alpha}_t = \prod_{s=1}^t (1 - \beta_s)$ . The noise estimator  $\epsilon_\theta(\cdot)$  in Eq. (10) is usually implemented by a U-Net [52], whose encoder converts the noisy image  $x_t$  into a latent feature  $f_{x,t}$ , and the decoder turns the combination of this feature as well as the time embedding  $f_t$ , i.e.  $f_{x,t} + f_t$ , back to the estimated noise. Although many other works also use conditions to control the diffusion models, they only integrate them during the generation phase, while the models are still unconditionally trained, which will compromise the models' capability of learning how to provide guides based on the extra conditions. Therefore, in our model, we also include the prompts and conditions in the training phase. Besides the time embedding  $f_t$ , we add the prompts embedding  $f_p$  and condition embedding  $f_d$  as extra channels into the hidden feature, i.e.  $f_{x,t} + f_t + f_p + f_d$ , before throwing it back to the U-Net decoder.

In real implementation, although the noise is gradually added during the diffusion process, it is proved to be equal to a one-step operation in Eq. (11). Therefore, from Eq. (10), during the training of previous diffusion models, an arbitrary  $t \in [1, T]$  is sampled and an accumulated noise is added according to Eq. (11), then the model is supposed to estimate this noise. In our design, since the total length of the diffusion process  $T_{cond}$  is dynamic, to better adapt to the change of diffusion steps, we also make some modification to the above training process. Specifically, for each target image  $x_0$  with prompts  $c_p$  and condition  $c_d$ , we first calculate the dynamic  $T_{cond}(c_p, c_d)$  as Eq. (5). In order to make our trained model more consistent with the dynamic diffusion process in the generation phase, we sample the  $t$  from the range  $[1, T_{cond}]$  that is adaptive to different target images to be generated. Besides, we make the reschedule for the noise parameters  $\{\beta'_1, \dots, \beta'_{T_{cond}}\}$  accordingly as introduced in Sec. 3.2.

In summary, the training process can be expressed by Algorithm. 1 and the training objective in our model can be rewritten as

$$\mathbb{E}_{t \in [1, T_{cond}(c_p, c_d)]} \|\epsilon_t - \epsilon_\theta(x_t, t, c_p, c_d)\|^2, \quad (12)$$

where

$$\begin{aligned} x_t &= \sqrt{\bar{\alpha}'_t} x_0 + \sqrt{1 - \bar{\alpha}'_t} \epsilon_t \\ &= \sqrt{\prod_{s=1}^t (1 - \beta'_s)} x_0 + \sqrt{1 - \prod_{s=1}^t (1 - \beta'_s)} \epsilon_t. \end{aligned} \quad (13)$$

---

#### Algorithm 1 Forward Diffusion Process

---

- 1: **given**  $x_0, c_p, c_d$
- 2: **repeat**
- 3:    $T_{cond} \leftarrow$  Eq. (5)
- 4:    $\{\beta'_1, \dots, \beta'_{T_{cond}}\} \leftarrow$  Eq. (7) – Eq. (9)
- 5:    $t \sim \{1, \dots, T_{cond}\}$
- 6:    $\epsilon \sim \mathcal{N}(\mathbf{0}, \mathbf{I})$
- 7:   Take gradient descent step on

$$\nabla_\theta \|\epsilon - \epsilon_\theta(\sqrt{\bar{\alpha}'_t} x_0 + \sqrt{1 - \bar{\alpha}'_t} \epsilon, t, c_p, c_d)\|^2$$

- 8: **until** converged

---

### 3.4 Generation Phase – Reverse Diffusion Process

During the generation process, the model is given the priors of what is going to be generated and how it should look like through text descriptions and additional conditions, such as sketch, input by users. Our model first estimates the adaptive length  $T_{cond}$  of the reverse diffusion process needed for generating the required high-quality image, which is controlled by prompts  $c_p$  and conditions  $c_d$ . Given an initial state  $x_{T_{cond}} \sim \mathcal{N}(\mathbf{0}, \mathbf{I})$ , the generation process takes a sample in each step from the denoised output, which can be also regarded as a Gaussian distribution, i.e.

$$x_{t-1} \sim \mathcal{N}(\mu_\theta(x_t, t, c_p, c_d), \beta'_t \mathbf{I}), \quad (14)$$

where

$$\begin{aligned} \boldsymbol{\mu}_\theta(x_t, t, c_p, c_d) &= \frac{1}{\sqrt{\alpha'_t}}(x_t - \frac{\beta'_t}{\sqrt{1 - \bar{\alpha}'_t}}\epsilon_\theta(x_t, t, c_p, c_d)), \\ \alpha'_t &= 1 - \beta'_t, \quad \bar{\alpha}'_t = \prod_{s=1}^t \alpha'_s. \end{aligned} \quad (15)$$

We can also simplify the Eq. (14) - (15) by computing

$$x_{t-1} = \frac{1}{\sqrt{\alpha'_t}}(x_t - \frac{\beta'_t}{\sqrt{1 - \bar{\alpha}'_t}}\epsilon_\theta(x_t, t, c_p, c_d)) + \sqrt{\beta'_t}z, \quad (16)$$

where  $z \sim \mathcal{N}(\mathbf{0}, \mathbf{I})$ . The whole process can be summarized as Algorithm. 2.

---

**Algorithm 2** Reverse Diffusion Process

---

```

1: given  $c_p, c_d$ 
2:  $T_{cond} \leftarrow Eq. (5)$ 
3:  $\{\beta'_1, \dots, \beta'_{T_{cond}}\} \leftarrow Eq. (7) - Eq. (9)$ 
4:  $x_{T_{cond}} \sim \mathcal{N}(\mathbf{0}, \mathbf{I})$ 
5: for  $t = T_{cond}, \dots, 1$  do
6:    $z \sim \mathcal{N}(\mathbf{0}, \mathbf{I})$  if  $t > 1$  else  $z = 0$ 
7:    $x_{t-1} \leftarrow Eq. (16)$ 
8: end for
9: return  $x_0$ 

```

---

## 4 Experiment

### 4.1 Experimental Setup

#### 4.1.1 Datasets

- **Cifar-10** [53]: Cifar-10 contains 60000 real images of 10 categories, each one of them is a  $32 \times 32$  color image. The dataset is pre-divided into the training and testing set with the ratio as 5 : 1. In our experiments, we take the category name of each image as the text prompt, and the corresponding edge map as the additional condition to control the generation. The generation evaluation is conducted on the testing set of it.

#### 4.1.2 Evaluation Metrics

The evaluation of our model includes two aspects: 1) generated image quality, which can be categorized into the following metrics: *Fréchet Inception Distance (FID,  $\downarrow$ )* [54], *CLIP Score (C-Score,  $\uparrow$ )* [55] and *CLIP Aesthetic Score (C-Aes.,  $\uparrow$ )* [56]. 2) generation efficiency, including *Average Diffusion Time-Steps (#Steps,  $\downarrow$ )* and *Average Execution Time (Time,  $\downarrow$ )*.

#### 4.1.3 Implementation Details

In our implementation, we assume that the text prompts mainly constrain the target category to be generated, and the input condition provides a spatial clue about an expected image. To realize these functions, the text prompts we used are category names and image conditions are edge maps to mimic the sketch given by users. To embed these two inputs, we utilize the text and image encoders of a pre-trained CLIP-ViT-B/32 model. The other newly-added modules, including the cross-model fusion in CTS and the combination parameter learner in AHNS, are implemented by two-layer MLP models with sigmoid activation. Besides our AC-Diff, all the models applied in experiments are trained from scratch with  $500k$  iterations using the batch-size 96 and also tested on a single RTX-4090 GPU.

### 4.2 Overall Performance

The overall comparison among different diffusion-based generative models is given in Table. 1. Since our model is built based on DDPM [16], we also include the unconditional diffusion models, DDPM [5] and DDIM, into our comparison as a reference. In order to add conditional control to these models, different from conventional studies, the extra text prompts and image conditions are not only fed into the pre-trained unconditional models during the generation process

Table 1: Overall comparison among different methods on Cifar-10.

Method	FID ( $\downarrow$ )	C-Score-t2i ( $\uparrow$ )	C-Score-i2i ( $\uparrow$ )	C-Aes. ( $\uparrow$ )	#Steps ( $\downarrow$ )	Time ( $\downarrow$ )
Original Image	-	0.2539	0.7896	3.7259	-	-
Unconditional Models						
DDPM [5]	29.5955	0.2110	0.7658	3.5850	1000	15.1748
DDIM [16]	29.6106	0.2124	0.7678	3.6739	1000	16.4451
	30.9802	0.2136	0.7632	3.6609	100	1.1036
	32.2251	0.2160	0.7633	3.6106	50	0.5600
Conditional Models						
DDPM (cond r.)	32.1141	0.2115	0.7703	3.5380	1000	12.9505
DDIM (cond r.)	34.6714	0.2118	0.7680	3.6720	1000	16.1519
	34.0696	0.2125	0.7752	3.6640	100	1.3377
	33.3599	0.2140	0.7670	3.6298	50	0.7521
DDPM* (cond f.&r.)	28.4607	0.2546	<b>0.7955</b>	3.5899	1000	17.4065
DDIM* (cond f.&r.)	28.6429	0.2528	0.7948	3.7101	1000	18.4088
	29.0791	0.2556	0.7913	3.7087	100	1.9522
	29.6803	<b>0.2575</b>	0.7898	3.6722	50	0.9958
Guided-Diffusion (DDPM) [6]	42.4932	0.2527	0.7752	3.1055	250	8.8107
Guided-Diffusion (DDIM) [6]	34.2655	0.2348	0.7719	3.5243	25	0.8431
SDG [10]	30.2310	0.2122	0.7696	3.4599	1000	55.0681
AC-Diff	<b>22.4677</b>	0.2545	0.7933	<b>3.7664</b>	141	2.0376

(noted as DDPM (cond r.) and DDIM (cond r.)), but are also incorporated into the training phase of these models. The models obtained in the latter case are denoted as DDPM\* (cond f.&r.) and DDIM\* (cond f.&r.). Besides, we also take some representative and popular conditional diffusion models into consideration, including Guided-Diffusion [6] and SDG [10]. During experiments, we generate  $2.5k$  images (about 1/4 of the number of samples in the full test set, and evaluate each of them. As seen from the table, our model can greatly reduce the average number of steps needed for conditional image generation as well as maintain the comparable quality of the generated images compared with the models which take a large number of steps in their diffusion processes.

### 4.3 Ablation Study

In the remaining of this section, we will discuss the effectiveness of each component in our model according to the experimental performance, including *conditional training*, *dynamic time-step* and *adaptive noise rescheduling*.

- **Conditional Training:** In Table. 1, by comparing the performance among DDPM, DDIM and their variants DDPM (cond r.), DDIM (cond r.), we find that using a pre-trained unconditional model and only directly adding extra conditions during generation, as commonly did in most previous conditional models, is not a good idea. The slight increase of CLIP Score, which represents the correlations among generated images and given conditions, is not comparable to the large decrease of the realism of image generated, reflecting in the reduction of FID and CLIP Aesthetic Score. The most important reason is that these models don't learn how to utilize the given conditions in their training phase. Instead, after we also integrate extra prompts and conditions into the training phase, and teach them how to be controlled by these clues, as did in DDPM\* (cond f.&r.) and DDIM\* (cond f.&r.), the models improve both the condition-correlations and the image qualities.
- **Dynamic Time-Step:** Through experiments, our AC-Diff can use much fewer diffusion steps to generate images with the same level qualities. It proves that a fixed large number of steps is not always necessary. Besides, we find that blindly reducing the generation steps to the same number for all kinds of images will hurt the quality of them. Instead, adaptively deciding the steps is much more effective. To better illustrate such an adaption, we list the category-level average steps required for generation in Fig. 5.
- **Adaptive Noise Rescheduling:** The generation process of any diffusion model starts from a total Gaussian noise each time, and gradually removes noise at each step. Since the total number of steps we used for generation are adaptive, the noise ratios cannot be the same for different generation tasks. Intuitively, the fewer the number of steps taken, the more noise should be removed at each step. To evaluate our design, we also compare the performance of AC-Diff models with different noise scheduling, including 1) the fully-adaptive noise ratios and 2) directly downsampling from pre-calculated noise ratios. The results are shown in Table. 2, and the fully-adaptive one outperforms the other.

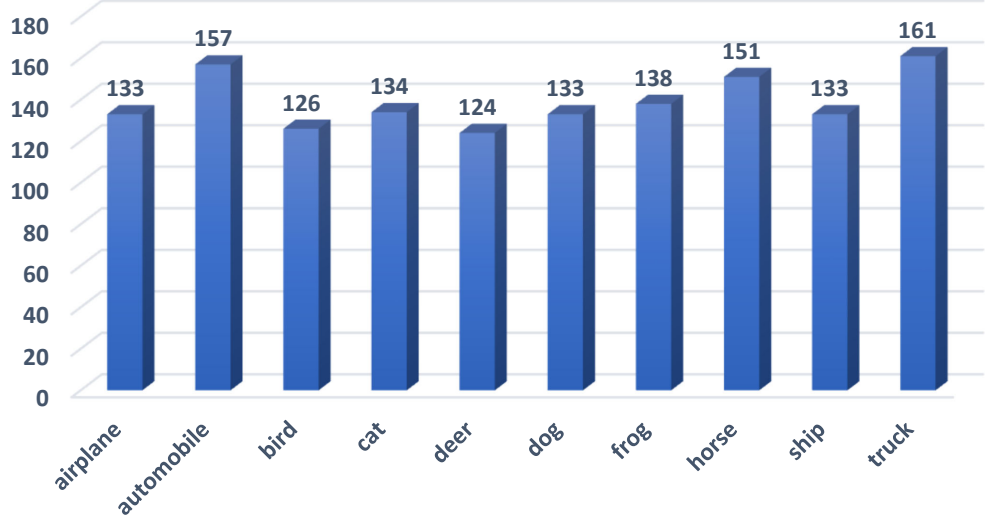


Figure 5: Category-level average number of diffusion steps needed in Cifar-10

Table 2: Performance of AC-Diff with different noise reschedule strategies.

Method	FID	C-Score-t2i	C-Score-i2i	C-Aes.
Fixed- $\beta$	47.2681	0.2499	0.7927	2.9297
Adaptive- $\beta$	22.4677	0.2545	0.7933	3.7664

#### 4.4 Qualitative Study

To better illustrate the generation performance, we give some examples of images generated by our method in Fig. 6. In general, the quality of adaptively generated images is generally satisfactory with recognizable contents.

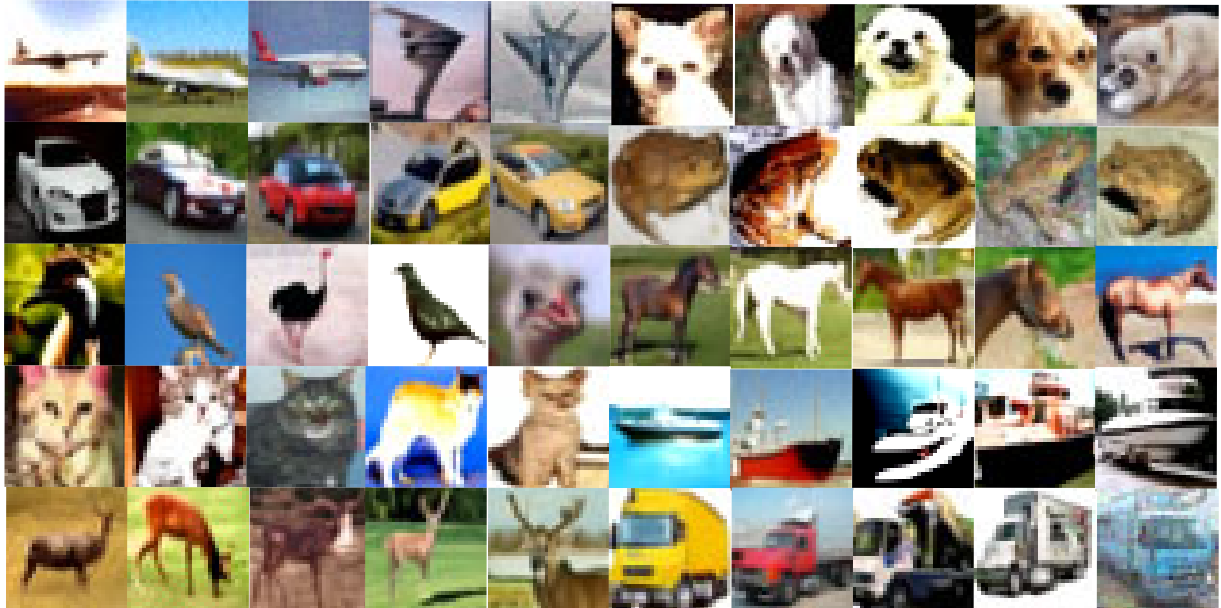


Figure 6: Examples of generated images using AC-Diff.

## 5 Conclusion

In this paper, we propose a new adaptive diffusion framework. Different from previous methods which commonly follow a fixed diffusion process, our model first estimates the number of diffusion steps needed according to the input prompts and additional conditions to estimate the complexity of the image to generate, based on which the number of steps needed for the diffusion is determined. In addition, we replace the commonly used pre-defined noise schedule, which is parameterized by diffusion rates, with a hybrid re-schedule module. By doing so, our model can largely reduce the computation when it is unnecessary while adding extra diffusion steps for a complex generation task to keep its performance. Through experiments, our method is proved to be able to keep the same generation quality with much less average calculation and execution time than those from the literature work. In the future, we will also apply our method to more complicated real-world data to test its effectiveness.

## References

- [1] Yoshua Bengio, Réjean Ducharme, and Pascal Vincent. A neural probabilistic language model. In T. Leen, T. Dietterich, and V. Tresp, editors, *Advances in Neural Information Processing Systems*, volume 13. MIT Press, 2000.
- [2] George Papamakarios, Eric Nalisnick, Danilo Jimenez Rezende, Shakir Mohamed, and Balaji Lakshminarayanan. Normalizing flows for probabilistic modeling and inference. *Journal of Machine Learning Research*, 22(57):1–64, 2021.
- [3] Diederik P. Kingma and Max Welling. Auto-Encoding Variational Bayes. In *2nd International Conference on Learning Representations, ICLR 2014, Banff, AB, Canada, April 14–16, 2014, Conference Track Proceedings*, 2014.
- [4] Ian Goodfellow, Jean Pouget-Abadie, Mehdi Mirza, Bing Xu, David Warde-Farley, Sherjil Ozair, Aaron Courville, and Yoshua Bengio. Generative adversarial nets. In Z. Ghahramani, M. Welling, C. Cortes, N. Lawrence, and K.Q. Weinberger, editors, *Advances in Neural Information Processing Systems*, volume 27. Curran Associates, Inc., 2014.
- [5] Jonathan Ho, Ajay Jain, and Pieter Abbeel. Denoising diffusion probabilistic models. In H. Larochelle, M. Ranzato, R. Hadsell, M.F. Balcan, and H. Lin, editors, *Advances in Neural Information Processing Systems*, volume 33, pages 6840–6851. Curran Associates, Inc., 2020.
- [6] Prafulla Dhariwal and Alexander Quinn Nichol. Diffusion models beat GANs on image synthesis. In A. Beygelzimer, Y. Dauphin, P. Liang, and J. Wortman Vaughan, editors, *Advances in Neural Information Processing Systems*, 2021.
- [7] Jonathan Ho and Tim Salimans. Classifier-free diffusion guidance. In *NeurIPS 2021 Workshop on Deep Generative Models and Downstream Applications*, 2021.
- [8] Alex Nichol, Prafulla Dhariwal, Aditya Ramesh, Pranav Shyam, Pamela Mishkin, Bob McGrew, Ilya Sutskever, and Mark Chen. Glide: Towards photorealistic image generation and editing with text-guided diffusion models. *arXiv preprint arXiv:2112.10741*, 2021.
- [9] Wei Li, Xue Xu, Xinyan Xiao, Jiachen Liu, Hu Yang, Guohao Li, Zhanpeng Wang, Zhifan Feng, Qiaoqiao She, Yajuan Lyu, and Hua Wu. Upainting: Unified text-to-image diffusion generation with cross-modal guidance. *arXiv:2210.16031 [cs.CV]*, 2022.
- [10] Xihui Liu, Dong Huk Park, Samaneh Azadi, Gong Zhang, Arman Chopikyan, Yuxiao Hu, Humphrey Shi, Anna Rohrbach, and Trevor Darrell. More control for free! image synthesis with semantic diffusion guidance. In *Proceedings of the IEEE/CVF Winter Conference on Applications of Computer Vision (WACV)*, pages 289–299, January 2023.
- [11] Andrey Voynov, Kfir Aberman, and Daniel Cohen-Or. Sketch-guided text-to-image diffusion models. In *ACM SIGGRAPH 2023 Conference Proceedings, SIGGRAPH '23, New York, NY, USA, 2023*. Association for Computing Machinery.
- [12] Ling Yang, Zhilin Huang, Yang Song, Shenda Hong, Guohao Li, Wentao Zhang, Bin Cui, Bernard Ghanem, and Ming-Hsuan Yang. Diffusion-based scene graph to image generation with masked contrastive pre-training. *arXiv preprint arXiv:2211.11138*, 2022.
- [13] Guangcong Zheng, Xianpan Zhou, Xuewei Li, Zhongang Qi, Ying Shan, and Xi Li. Layoutdiffusion: Controllable diffusion model for layout-to-image generation. In *Proceedings of the IEEE/CVF Conference on Computer Vision and Pattern Recognition (CVPR)*, pages 22490–22499, June 2023.

[14] Alexander Quinn Nichol and Prafulla Dhariwal. Improved denoising diffusion probabilistic models. In Marina Meila and Tong Zhang, editors, *Proceedings of the 38th International Conference on Machine Learning*, volume 139 of *Proceedings of Machine Learning Research*, pages 8162–8171. PMLR, 18–24 Jul 2021.

[15] Daniel Watson, Jonathan Ho, Mohammad Norouzi, and William Chan. Learning to efficiently sample from diffusion probabilistic models. 2022.

[16] Jiaming Song, Chenlin Meng, and Stefano Ermon. Denoising diffusion implicit models. In *International Conference on Learning Representations*, 2021.

[17] Daniel Watson, William Chan, Jonathan Ho, and Mohammad Norouzi. Learning fast samplers for diffusion models by differentiating through sample quality. In *International Conference on Learning Representations*, 2022.

[18] Robin San-Roman, Eliya Nachmani, and Lior Wolf. Noise estimation for generative diffusion models. 2021.

[19] Hyungjin Chung, Byeongsu Sim, and Jong Chul Ye. Come-closer-diffuse-faster: Accelerating conditional diffusion models for inverse problems through stochastic contraction. In *Proceedings of the IEEE/CVF Conference on Computer Vision and Pattern Recognition (CVPR)*, pages 12413–12422, June 2022.

[20] Zhaoyang Lyu, Xudong XU, Ceyuan Yang, Dahua Lin, and Bo Dai. Accelerating diffusion models via early stop of the diffusion process. 2022.

[21] Huangjie Zheng, Pengcheng He, Weizhu Chen, and Mingyuan Zhou. Truncated diffusion probabilistic models and diffusion-based adversarial auto-encoders. In *The Eleventh International Conference on Learning Representations*, 2023.

[22] Zebin You, Yong Zhong, Fan Bao, Jiacheng Sun, Chongxuan Li, and Jun Zhu. Diffusion models and semi-supervised learners benefit mutually with few labels. 2023.

[23] Shuyang Gu, Dong Chen, Jianmin Bao, Fang Wen, Bo Zhang, Dongdong Chen, Lu Yuan, and Baining Guo. Vector quantized diffusion model for text-to-image synthesis. In *Proceedings of the IEEE/CVF Conference on Computer Vision and Pattern Recognition (CVPR)*, pages 10696–10706, June 2022.

[24] Chitwan Saharia, William Chan, Saurabh Saxena, Lala Li, Jay Whang, Emily Denton, Seyed Kamyar Seyed Ghasemipour, Raphael Gontijo-Lopes, Burcu Karagol Ayan, Tim Salimans, Jonathan Ho, David J. Fleet, and Mohammad Norouzi. Photorealistic text-to-image diffusion models with deep language understanding. In Alice H. Oh, Alekh Agarwal, Danielle Belgrave, and Kyunghyun Cho, editors, *Advances in Neural Information Processing Systems*, 2022.

[25] Aditya Ramesh, Prafulla Dhariwal, Alex Nichol, Casey Chu, and Mark Chen. Hierarchical text-conditional image generation with clip latents. *ArXiv*, abs/2204.06125, 2022.

[26] Omri Avrahami, Thomas Hayes, Oran Gafni, Sonal Gupta, Yaniv Taigman, Devi Parikh, Dani Lischinski, Ohad Fried, and Xi Yin. Spatext: Spatio-textual representation for controllable image generation. In *Proceedings of the IEEE/CVF Conference on Computer Vision and Pattern Recognition*, pages 18370–18380, 2023.

[27] Jiwen Yu, Yinhui Wang, Chen Zhao, Bernard Ghanem, and Jian Zhang. Freedom: Training-free energy-guided conditional diffusion model. *Proceedings of the IEEE/CVF International Conference on Computer Vision (ICCV)*, 2023.

[28] Georgios Batzolis, Jan Stanczuk, Carola-Bibiane Schönlieb, and Christian Etmann. Conditional image generation with score-based diffusion models. *arXiv:2111.13606 [cs.LG]*, 2021.

[29] Lvmin Zhang, Anyi Rao, and Maneesh Agrawala. Adding conditional control to text-to-image diffusion models. In *IEEE International Conference on Computer Vision (ICCV)*, 2023.

[30] Can Qin, Shu Zhang, Ning Yu, Yihao Feng, Xinyi Yang, Yingbo Zhou, Huan Wang, Juan Carlos Niebles, Caiming Xiong, Silvio Savarese, et al. Unicontrol: A unified diffusion model for controllable visual generation in the wild. *arXiv preprint arXiv:2305.11147*, 2023.

[31] Alec Radford, Jong Wook Kim, Chris Hallacy, Aditya Ramesh, Gabriel Goh, Sandhini Agarwal, Girish Sastry, Amanda Askell, Pamela Mishkin, Jack Clark, Gretchen Krueger, and Ilya Sutskever. Learning transferable visual models from natural language supervision. In Marina Meila and Tong Zhang, editors, *Proceedings of the 38th International Conference on Machine Learning*, volume 139 of *Proceedings of Machine Learning Research*, pages 8748–8763. PMLR, 18–24 Jul 2021.

[32] Robin Rombach, Andreas Blattmann, Dominik Lorenz, Patrick Esser, and Björn Ommer. High-resolution image synthesis with latent diffusion models. In *Proceedings of the IEEE/CVF Conference on Computer Vision and Pattern Recognition (CVPR)*, pages 10684–10695, June 2022.

[33] Vedant Singh, Surgan Jandial, Ayush Chopra, Siddharth Ramesh, Balaji Krishnamurthy, and Vineeth N. Balasubramanian. On conditioning the input noise for controlled image generation with diffusion models. 2022.

[34] Zijian Zhang, Zhou Zhao, Jun Yu, and Qi Tian. Shiftddpms: Exploring conditional diffusion models by shifting diffusion trajectories. *arXiv preprint arXiv:2302.02373*, 2023.

[35] Yang Song and Stefano Ermon. Generative modeling by estimating gradients of the data distribution. In H. Wallach, H. Larochelle, A. Beygelzimer, F. d’Alché-Buc, E. Fox, and R. Garnett, editors, *Advances in Neural Information Processing Systems*, volume 32. Curran Associates, Inc., 2019.

[36] Yang Song, Jascha Sohl-Dickstein, Diederik P Kingma, Abhishek Kumar, Stefano Ermon, and Ben Poole. Score-based generative modeling through stochastic differential equations. In *International Conference on Learning Representations*, 2021.

[37] Tero Karras, Miika Aittala, Timo Aila, and Samuli Laine. Elucidating the design space of diffusion-based generative models. In Alice H. Oh, Alekh Agarwal, Danielle Belgrave, and Kyunghyun Cho, editors, *Advances in Neural Information Processing Systems*, 2022.

[38] Qinsheng Zhang and Yongxin Chen. Fast sampling of diffusion models with exponential integrator. In *The Eleventh International Conference on Learning Representations*, 2023.

[39] Cheng Lu, Yuhao Zhou, Fan Bao, Jianfei Chen, Chongxuan Li, and Jun Zhu. DPM-solver: A fast ODE solver for diffusion probabilistic model sampling in around 10 steps. In Alice H. Oh, Alekh Agarwal, Danielle Belgrave, and Kyunghyun Cho, editors, *Advances in Neural Information Processing Systems*, 2022.

[40] Alexia Jolicoeur-Martineau, Ke Li, Rémi Piché-Taillefer, Tal Kachman, and Ioannis Mitliagkas. Gotta go fast when generating data with score-based models. *arXiv preprint arXiv:2105.14080*, 2021.

[41] Qinsheng Zhang, Molei Tao, and Yongxin Chen. gDDIM: Generalized denoising diffusion implicit models. In *The Eleventh International Conference on Learning Representations*, 2023.

[42] Luping Liu, Yi Ren, Zhijie Lin, and Zhou Zhao. Pseudo numerical methods for diffusion models on manifolds. In *International Conference on Learning Representations*, 2022.

[43] Tim Dockhorn, Arash Vahdat, and Karsten Kreis. Score-based generative modeling with critically-damped langevin diffusion. In *International Conference on Learning Representations (ICLR)*, 2022.

[44] Eric Luhman and Troy Luhman. Knowledge distillation in iterative generative models for improved sampling speed. 2021.

[45] Tim Salimans and Jonathan Ho. Progressive distillation for fast sampling of diffusion models. In *International Conference on Learning Representations*, 2022.

[46] Chenlin Meng, Robin Rombach, Ruiqi Gao, Diederik Kingma, Stefano Ermon, Jonathan Ho, and Tim Salimans. On distillation of guided diffusion models. In *Proceedings of the IEEE/CVF Conference on Computer Vision and Pattern Recognition (CVPR)*, pages 14297–14306, June 2023.

[47] Alexey Dosovitskiy, Lucas Beyer, Alexander Kolesnikov, Dirk Weissenborn, Xiaohua Zhai, Thomas Unterthiner, Mostafa Dehghani, Matthias Minderer, Georg Heigold, Sylvain Gelly, Jakob Uszkoreit, and Neil Houlsby. An image is worth 16x16 words: Transformers for image recognition at scale. In *International Conference on Learning Representations*, 2021.

[48] Kieran G Larkin. Reflections on shannon information: In search of a natural information-entropy for images. *arXiv preprint arXiv:1609.01117*, 2016.

[49] Yue Wu, Yicong Zhou, George Saveriades, Sos Agaian, Joseph P Noonan, and Premkumar Natarajan. Local shannon entropy measure with statistical tests for image randomness. *Information Sciences*, 222:323–342, 2013.

[50] Marius Vila, Anton Bardera, Miquel Feixas, Philippe Bekaert, and Mateu Sbert. Analysis of image informativeness measures. In *2014 IEEE International Conference on Image Processing (ICIP)*, pages 1086–1090. IEEE, 2014.

[51] Jascha Sohl-Dickstein, Eric Weiss, Niru Maheswaranathan, and Surya Ganguli. Deep unsupervised learning using nonequilibrium thermodynamics. In Francis Bach and David Blei, editors, *Proceedings of the 32nd International Conference on Machine Learning*, volume 37 of *Proceedings of Machine Learning Research*, pages 2256–2265, Lille, France, 07–09 Jul 2015. PMLR.

[52] Olaf Ronneberger, Philipp Fischer, and Thomas Brox. U-net: Convolutional networks for biomedical image segmentation. In Nassir Navab, Joachim Hornegger, William M. Wells, and Alejandro F. Frangi, editors, *Medical Image Computing and Computer-Assisted Intervention – MICCAI 2015*, pages 234–241, Cham, 2015. Springer International Publishing.

[53] Alex Krizhevsky, Vinod Nair, and Geoffrey Hinton. Cifar-10 (canadian institute for advanced research).

- [54] Martin Heusel, Hubert Ramsauer, Thomas Unterthiner, Bernhard Nessler, and Sepp Hochreiter. Gans trained by a two time-scale update rule converge to a local nash equilibrium. In I. Guyon, U. Von Luxburg, S. Bengio, H. Wallach, R. Fergus, S. Vishwanathan, and R. Garnett, editors, *Advances in Neural Information Processing Systems*, volume 30. Curran Associates, Inc., 2017.
- [55] Alec Radford, Jong Wook Kim, Chris Hallacy, Aditya Ramesh, Gabriel Goh, Sandhini Agarwal, Girish Sastry, Amanda Askell, Pamela Mishkin, Jack Clark, Gretchen Krueger, and Ilya Sutskever. Learning transferable visual models from natural language supervision. In Marina Meila and Tong Zhang, editors, *Proceedings of the 38th International Conference on Machine Learning*, volume 139 of *Proceedings of Machine Learning Research*, pages 8748–8763. PMLR, 18–24 Jul 2021.
- [56] Christoph Schuhmann, Romain Beaumont, Richard Vencu, Cade W Gordon, Ross Wightman, Mehdi Cherti, Theo Coombes, Aarush Katta, Clayton Mullis, Mitchell Wortsman, Patrick Schramowski, Srivatsa R Kundurthy, Katherine Crowson, Ludwig Schmidt, Robert Kaczmarczyk, and Jenia Jitsev. LAION-5b: An open large-scale dataset for training next generation image-text models. In *Thirty-sixth Conference on Neural Information Processing Systems Datasets and Benchmarks Track*, 2022.